Facile Fabrication of MoS_2/ZnO Hetero-Epitaxial Growth on Cu_2O with Enhanced Photoelectrochemical Activity Through Thermal Oxidation Process

M. Abdurrahman[1], F.W Burari[2], O.W Olasoji[2],

[1] Department of physics, faculty of Natural science, Federal University Dutse, Jigawa State, Nigeria,
[2] Department of physics, faculty of Natural science, Abubakar Tafawa Balewa University, Bauchi state, Nigeria,

*Corresponding author; Email: msabduurahman@yahoo.com.

Article Info

Article history:

Received , 17/06/2023
Revised, , 06/08/2023
Accepted , 07/12/2023

Keywords:

Thermal oxidation
annealing
photoelectrochemical
cuprous oxide
etching

ABSTRACT

A succession of novel heteroepitaxial grown hybrid films MoS_2 and ZnO thin film composites have been effectually synthesized on Cu_2O by a two-step thermal oxidation method for efficient photoelectrochemical processes and analyzed by X-ray diffraction (XRD), Ftir investigations, and they were characterized by photoelectrochemical analysis and confirmed their Successful synthesis. In this unparalleled strategy, two semiconductors are sandwiched between three-dimensional Cu_2O substrates to provide numerous active sites for photocatalytic oxidation improve noticeable light absorption and restrain photogenic charge reunification. Therefore, the resulting fabricated hybrid (ZnO/Cu_2O/MoS_2) acts as a direct working electrode and is highly reactive in water by the PEC process, which can facilitate the estrangement of photogenerated electron-hole twosomes below low realistic voltage. Therefore, the photocurrent response of the fabricated ZnO/Cu_2O/MoS_2 working electrode was appreciably enhanced due to the synergistic effect of every element of the 3D structure. Consequently, the produced photoelectrochemical cell showed high sensitivity with wattage conversion efficiency (PCE) of 0.30%, an open circuit voltage (Voc) of 38 mV, and a short circuit current density (I_{SC}) of 0.66 mA.

I. Introduction

Semiconductor-build photocatalyst Zinc oxide (ZnO) as an auspicious has been broadly examined for removing carbon-based contaminants in water due to its radiosensitivity, soaring thermal steadiness, economical or low-priced, and environmental sociability [1]. Nevertheless, under visible light irradiation the extensive bandgap of ZnO limits its photocatalytic activity and its high electron-hole reunification rate was due to the high exciton binding energy [2]. Coalesce ZnO with bimetallic or monometallic noble metals for instance ag, au, pt, auag and aupd infinitesimal particles has been proposed the localized surface plasmon resonance effect to extend the optical absorption bandwidth of ZnO, this is one of the recommended resolutions used for extending the optical incorporation bandwidth. At the interfaces between ZnO and magnanimous metals that yield the formation schottky junctions can also efficiently augment the photocatalytic bustle and detached the photogenerated charges of pure zinc oxide [3–9]. On the other hand, the practical application of this material extrammel by these high-priced precious metals [10]. Therefore, another procedure or method is to merge relatively narrow bandgap semiconductors with ZnO. This also effectively separating

electrons and holes, at the same time widen the optical absorption bandwidth, [11]. In recent years, transition metal dichalcogenides (tmds) have attracted much attention as new materials for photocatalysis for instance WS_2, MoS_2, $MoSe_2$ and WSe_2 [12,13]. Molybdenum disulphide (MoS_2) is one of the most intensively studied tmds due to its highly photochemical properties, electrical and tunable optical. The molybdenum disulphide (MoS_2) has a graphene-alike physical composition of prearranged coatings clutched together by van der waals forces. These tmds are in the hexangular family, although be different in the number of coatings [13], the main MoS_2 epitomes are single-coating1t (trigonal) and 1h (hexagonal) diamond dust systems, two-layer hexangular 2h and three-coating rhombohedral 3r. Amongst them, the 1t phase is octahedrally synchronized and metastable [10,13]. MoS_2 when its dimension is abridged to a two-dimensional structure has a diminutive tortuous bandgap (1.3 ev) in bulk and a larger direct bandgap (1.9 ev). Accordingly, low-multidimensional MoS_2 is well-thought-out as a hopeful visible-light photocatalyst that can bind with ZnO [11,14–20]. In the decomposition of rhodamine b and methylene blue MoS_2 was studied as a cocatalyst for ZnO and the outcomes displayed that the photocatalytic effectiveness of ZnO/MoS_2 was improved due to broadened light absorption window, enhanced charge separation and increased active sites [11,14–20]. Computational studies show that the configuration of the ZnO/MoS_2 heterostructure narrows the bandgap, promotes the separation of photogenerated excitons, at the boundary creates a large built-in electric field and broadens the incorporation range [21,22].

Amongst an assortment p-type semiconductors, copper oxide (Cu_2O) with an unwavering bandgap of 2.0 ev has emerged as a hopeful photocathode material [23-26], which can be used for solar energy conversion, spontaneous generation, water splitting, and efficient photocathode materials, sensing [27-31], as a result of its advantages such as low toxicity and light absorption. On the other hand, attributable to its soaring charge reunification rate the production of copper ii oxide (CuO) was still limited. Cu_2O with an arrayed three-dimensional (3d) structure can, provide more reactive sites, increase the specific surface area, resulting in a significantly minimized carrier diffusion length, and offer advantages for direct electron transfer further improving the pec properties and response [32-34].

In contrast, constructing heterojunction structures in other semiconducting materials has also been an effective approach [35-38]. Here, an n-type ZnO semiconducting material with a conduction band that maintains band meandering in cu_2o was preferred. The formed band edge levels can enhanced well-organized separation of photoinduced electron-hole pairs, light absorption, and optoelectronic translation efficiency [27,39,40].

Copper i oxide (Cu_2O) is a hopeful semiconducting material as an optical material attributable to its suitable optical band configuration that response to the visible light spectral range. Cu_2O has valence and conduction bands and can oxidize and reduce water to hydrogen and oxygen. Cu_2O, a p-type semiconducting material with a bandgap of 2.1 ev and conductivity, is widely used in many implementations attributable to its soaring-performance conversion of solar energy, high absorption coefficient and excellent photocatalytic properties to visible light [41-44]. Both zinc oxide (ZnO) and copper i oxide (Cu_2O) are natural materials low-cost, non-toxic. Zno and cu_2o can be formed using different methods [45-49]. The main approach in relation to this work is to connect a composite coat with metallic material ZnO accompanying a narrow bandgap semiconductor containing MoS_2. In this work, for the target of enhancing the photocatalytic capability of coated hybrid zno thin film composites, predominantly for exploiting the visible region of the solar spectrum we account an analysis on the synergistic function of MoS_2. We have constructively fabricated a succession of new thin-film heteroepitaxial composites, including ZnO/MoS_2 composites. The photoelectrochemical performance was evaluated by examining the PEC solar cells under sunlight irradiation. The fundamental features of these films were compared and investigated. The pec performance of cu_2o doped and MoS_2/ZnO electrodes were investigated and highest in rank operating electrode was determined.

II. Research Method

II.1 Synthesis of Cu_2O thin film

A small piece of Cu with a defined area (2 cm × 2 cm) was then thermally oxidized in a furnace. A commercially available pure copper (99.98%) sheet (0.1 mm thick) substrate was cut into small pieces (2 cm×2 cm). These copper foil pieces were washed with deionized (DI) water and dilute nitric acid for about 2 min, respectively, and subsequently dried in-between tissue paper for the removal of impurities on the film surface. The oxidation temperature was controlled over a wide range from room temperature (RT) to 450 °C. The heating pace was about 10 °C./min, and once the preferred maximum temperature was reached, it was held for 30 minutes to allow

copper oxide to form. After oxide formation, the furnace was allowed to cool for 2 hours. Slow cooling was maintained to minimize potential thermal stress and film cracking.

II.2 Synthesis of $MoS_2/ZnO/Cu_2O$ hybrid film

The arrangement used to evolve MoS_2 was chemical vapor deposition (CVD) [50, 51]. The Cu_2O substratum was subjected to a precise temperature and pressure conditions to chemically react with one or more precursors on the surface of the substratum to dummy up finest, big-region thin films. The appliance of chemical vapor deposition in sole-coating transition metal dichalcogenides (TMD) fabrication begins with the growth of MoS_2. The warming rate was set ahead at 10 °C for every minute and with an accession temperature of 650 °C and held at a temperature for thirty minute (30) minutes, the closure was open when the temperature drops to 400 °C. A MoS_2 configuration was acquired when the temperature was lowered to room temperature. The investigational procedure is revealed in Figure 1.0. CVD can efficiently produce single-layer and multilayer MoS_2/ZnO. We were able to grow high-superiority single-crystal stuffs and produce thin films consistently distributed over a outsized area. This was helpful in later fabrication of optoelectronic components.

Figure 1. Representation of a growing $MoS_2/ZnO/Cu_2O$ film.

II.3. PEC Measurement

In a crystal clear container the PEC pianism of the tailored operational electrode was cast about. For this purpose, two different electrode $MoS_2/ZnO/Cu_2O$ and Cu electrode were assembled and immersed in a crystal clear plastic container. To prepare the intermediate electrolyte, the 1g of NaCl powders were mixed with 25ml of distilled water, stirrer quietly in anticipation of the electrolyte to dissolve completely. The PEC performance of the hybrid electrodes was measured or evaluated using Current-Voltage measurements. The Photoelectrochemical studies were performed by means of a two-electrode electrochemical system. (Figure 2) show the graphic exemplification of photo bring forth charge carriers (e- & h+) after solar irradiation on the synthesized sample $MoS_2/ZnO/Cu_2O$. An operational electrode ($MoS_2/ZnO/Cu_2O$) and a copper (Cu) plate were employed as the counter electrodes, correspondingly. The multimeter was engaged to accomplished electrical path of the photocurrent density and photo voltage of electrodes under illumination (AM 1.5 G) within the potential window using 1g of NaCl electrolyte as a mediator between the two electrodes. The approach explained or expressed in this paper provides a simple and novel method to synthesize thin film materials, geared up for applicative applications for instance the photoelectrochemical solar cell and hydrogen production.

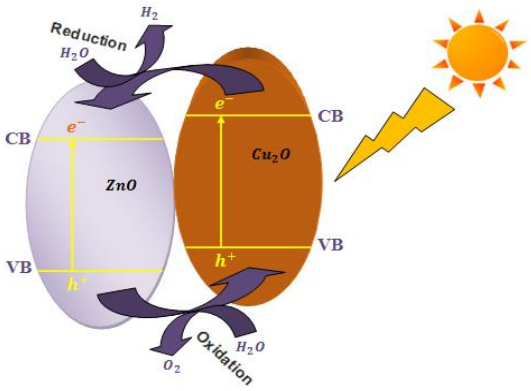

Figure 2: Schematic illustration of photo generated charge carriers (e- & h+) after solar irradiation on

II.4. XRD characterization of $MoS_2/ZnO/Cu_2O$

XRD pattern were made to examined or investigate the crystal phase and synthetic arrangement of the three dimensional (3D) Cu_2O on the copper (Cu) substrate. As guide physically in Fig. 3, dissemination peaks accompanying the horizontal in the (111), (200), and (220) bearings (noticeable with blueish trigon) at 43.8° and 51.2° maybe arranged to face- concentrated three dimensional copper substratum (JCPDS card No. 04-0836). Except for the optical phenomenon extremum above of the pure copper substrate, all supplementary diffraction extremum with the bearing in the (110), (111), (111), (200) and (220) corresponding to 29.7°, 36.6°, 37.0°, 42.2° and 61.7° maybe allotted to the three dimensional phase Cu_2O (JCPDS card No. 65-3288) [52,53,54,55], indicating the complete formation of Cu_2O with other impurities, such as CuO (111) at 38.9°[55]. Furthermore, to confirm or validate the sandwiched product of MoS_2/ZnO the XRD pattern was observed at 33.4°, 46.1°, 61.7° corresponding to (101), (104) and (008) correspondingly.

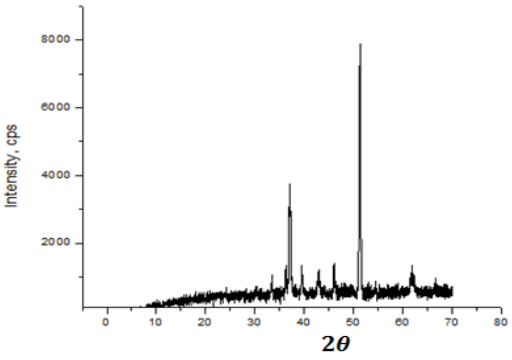

Figure 3. XRD pattern of MoS_2/ZnO/Cu_2O

II.5 FT-IR spectra analysis

As guide physically in Fig. 4 displayed the FTIR spectrum of doped Cu, Cu_2O stratum and MoS_2 thin coating and Fig. 5 represents the FTIR spectrum of MOS_2/ZnO/Cu_2O thin coatings. The FTIR extremum present in the spectrum fit into to Cu, ZnO, MoS_2 or Cu_2O forms. Numerous additional phases were detected or noticeable in the FTIR absorption spectrum. The FTIR absorption spectrum of $MoS_2/ZnO/Cu_2O$ thermally oxidized meant for 2h showed that ZnO, MoS_2 and Cu_2O phase was present in the details of the coating. In the range, a meaningful broad band in the range of 400-600, 700 cm^{-1} was ascribed to the dimension stretching trembling of the Zn-O chemical bond. The FTIR range of the film included three spectrum at 650, 620 and 2359 cm^{-1} tantamount to modes of zinc oxide [56,57]. In the FTIR spectra of the MoS_2 films doped with Cu_2O thermally oxidized for 2h, only the peaks in relating to ZnO, MoS_2 and Cu_2O were observed. The Cu_2O phase seemed at 615cm^{-1} doped with oxygen which was thermally oxidized for 2h. The peak at 2325cm^{-1} stands for the P-H modes. The peak at 3506cm^{-1} symbolize to the oxygen related compound modes of copper I oxide. This imperceptible peak 876-825cm^{-1} was certified to the archetypal distension trembling of the Cu(II)-O bond of copper I oxide setting [58,59]. As the oxidation point in time increased for conversion of Cu to Cu_2O, the intensity of copper I oxide increased. It was make known that the Cu_2O, MoS_2 segment set off forward when doped with ZnO at

altitudinous temperature. The peak at 3450cm^{-1} corresponded to the O-H modes, peak at 735cm^{-1} corresponded Benzene Ring, CH_2/CH_3 observed at 2900cm^{-1}[60, 61]. 998cm^{-1} are broad absorption bands attributed to MoS_2 [62, 63].

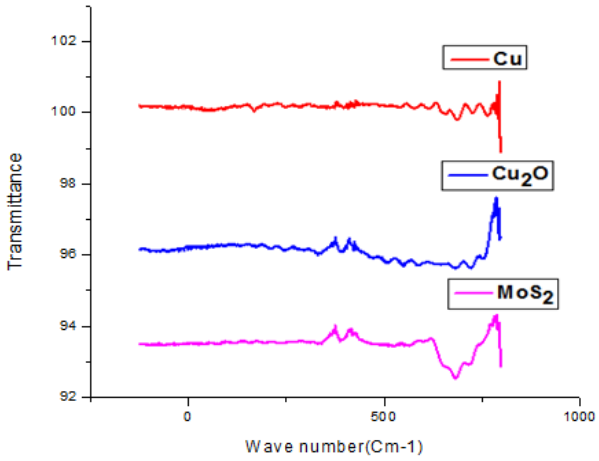

Fig. 4: Ftir Result of Cu, Cu_2O and MoS_2

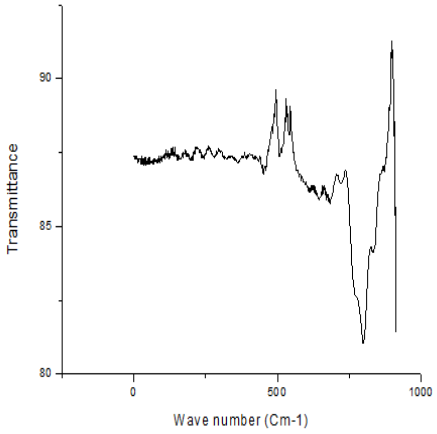

Fig. 5: MOS_2/ZnO/Cu_2O Ftir Result

II.6 I-V Curve analysis

The solar cells external parameters of the samples such as the efficiency, maximum power, photo voltage and photocurrent was obtained beneath illumination as delineated in Table 1.0 while the Cu- $ZnO/MoS_2/Cu_2O$ PEC solar cells were compared with characteristic curves for a set of exterior parametric quantity, pursued by modification power efficiency deduce from figure 6. When analyzing the prototype, the calculated external parameters of the organized samples Cu-Cu_2O and that of $ZnO/MoS_2/Cu_2O$ be stated as shown in table 1.0. To examined or investigate the solar cell parameters, two various readings are written utilizing a multimeter and abundant cosmic irradiances so that study the solar cell parametric quantity, two disparate graphs are premeditated for two different samples for examining the photo reaction and photo voltage of the working and counter electrode under illuminance. In table 1.0 it maybe visualized that for the analyzed $ZnO/MoS_2/Cu_2O$, the deposited of 2D materials and ZnO semiconductor material enhances the photo reaction simultaneously ever-increasing the efficiency of the model. It in addition acts at the same time as an absorption coating to engender charge carriers (electrons and holes) beneath solar radiation.

Table 1.0: The highest power, photocurrent, effectiveness and photo voltage of different reading of Cu-Cu_2O and Cu- $ZnO/MoS_2/Cu_2O$ photoelectrochemical solar cell

S/N	Sample	$I_{sc}(mA)$	$V_{oc}(mV)$	$\eta(\%)$
1	Cu_2O	0.13	10.0	0.035
2	MoS_2/ZnO	0.66	38	0.30

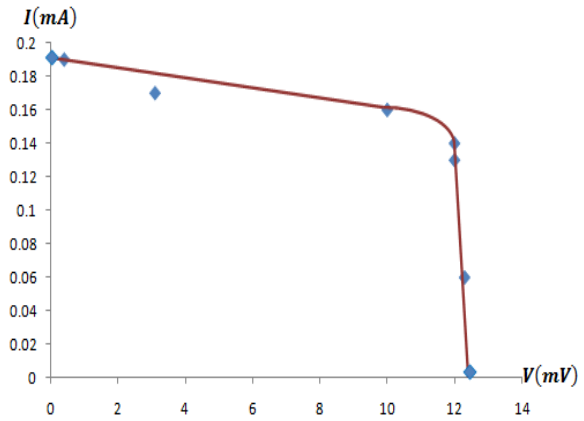

Fig 6: The graph of Cu-$ZnO/MoS_2/Cu_2O$ photoelectrochemical solar cell after surface modification

III. Conclusion

In summary, by combining layered ZnO and MoS_2, we have fruitfully synthesized a succession of novel heteroepitaxial compounds that display much higher photocatalytic activity than pure Cu_2O in photoelectrochemical solar cells under noticeable light irradiance. Both synergistic effects are correlated to the surface properties and visible light collection efficiency caused by the bonding of two different bandgap semiconducting materials. The arranged heteroepitaxial material showed increased activity towards increasing the power conversion efficiency of the engineered sample, about 9 times higher than pure Cu_2O. The means of transfer of the photo-generated electrons from ZnO to the MoS_2 facilitates an interfacial electron transfer and suppression of the recombination of charge carriers. Full structure and PEC analysis indicate that the enhanced PEC action possibly will be certified to the synergistic effect between the two 2D materials and semiconductor material. Moreover, the $ZnO/MoS_2/Cu_2O$ composites also showed good stability during the application of photoelectrochemical process. As a result, the use of Cu_2O as main substrate for ZnO/MoS_2 deposition as a new type of optoelectronic composite stuff put up a valuable candidate for photoelectrochemical solar cell and hydrogen production.

Acknowledgements

I would like to show gratitude TETFUND, Federal University Dutse, for providing favorable environment with free access to laboratory equipment during the research work.

References

[1] Kumar, S.G., Rao, K.S.R.K. (2015). Zinc oxide based photocatalysis: tailoring surface-bulk structure and related interfacial charge carrier dynamics for better environmental applications, RSC Adv. 5, 3306–3351, https://doi.org/10.1039/C4RA13299H.

[2] Liu, H.R., Shao, G.X., Zhao, J.F., Zhang, Z.X., Zhang, Y., Liang, J., Liu, X.G., Jia, H.S., Xu, B.S. (2012). Worm-like Ag/ZnO core-shell heterostructural composites: Fabrication, characterization, and photocatalysis, J Phys Chem C 116, 16182–16190, https://doi.org/10.1021/jp2115143.
[3] Vaiano, V., Jaramillo-Paez, C.A., Matarangolo, M., Navío, J.A., del Carmen Hidalgo, M. (2019). UV and visible-light driven photocatalytic removal of caffeine using ZnO modifed with different noble metals (Pt, Ag and Au), Mater Res Bull 112, 251–260, https://doi.org/10.1016/j.materresbull.2018.12.034.
[4] Mahardika, T., Putri, N.A., Putri, A.E., Fauzia, V., Roza, L., Sugihartono, I., Herbani, Y. (2019). Rapid and low temperature synthesis of Ag nanoparticles on the ZnO nanorods for photocatalytic activity improvement, Results Phys 13, 102209,, https://doi.org/10.1016/j.rinp.2019.102209.
[5] Arifn M., Roza, L., Fauzia, V., (2019). Bayberry-like Pt nanoparticle decorated ZnO nanorods for the photocatalytic application, Results Phys 15, 102678, , https://doi.org/10.1016/j.rinp.2019.102678.
[6] Jaramillo-Páez, C.A.A., Navío, J.A.A., Hidalgo, M.C.C., Macías, M. (2018). ZnO and Pt-ZnO photocatalysts: Characterization and photocatalytic activity assessing by means of three substrates, Catal Today 313, 12–19 https://doi.org/10.1016/j.cattod.2017.12.009.
[7] A. Ekaputri, V. Fauzia, L. Roza, Effect of Au nanoparticles and Au mesostars on the photocatalytic activity of ZnO nanorods, Mater Res Express 6 (2019) 84008, https://doi.org/10.1088/2053-1591/ab23aa.
[8] Lee, S.J., Jung, H.J., Koutavarapu, R., Lee, S.H., Arumugam, M., Kim, J.H. Choi, M.Y. (2019). ZnO supported Au/Pd bimetallic nanocomposites for plasmon improved photocatalytic activity for methylene blue degradation under visible light irradiation, Appl Surf Sci 496, 143665, , https://doi.org/10.1016/j.apsusc.2019.143665.
[9] Cheng, Y., Jiao, W. Q., Li, Y., Zhang, S., Li, D., Li, R., Che, (2018). Two hybrid Au-ZnO aggregates with different hierarchical structures : A comparable study in photocatalysis, J Colloid Interface Sci 509, 58–67, https://doi.org/10.1016/j.jcis.2017.08.077.
[10] Li, Z., Meng, X., Zhang, Z. (2018). Recent development on MoS2-based photocatalysis: A review, J Photochem Photobiol C Photochem Rev. 35, 39–55, https://doi.org/10.1016/j.jphotochemrev.2017.12.002.
[11] Kumar, S., Maivizhikannan, V., Drews, J., Krishnan, V. (2019). Fabrication of nanoheterostructures of boron doped ZnO-MoS_2 with enhanced photostability and photocatalytic activity for environmental remediation applications, Vacuum 163, 88–98, https://doi.org/10.1016/j.vacuum.2019.02.001.
[12] Hong, M., Wu, L., Li, N., Liu, D., jin Wang, Y. cheng Xue, Tang, L. (2018). Molybdenum disulfide (MoS_2) as a co-catalyst for photocatalytic degradation of organic contaminants: A review, Process Saf Environ Prot 118, 40–58, https://doi.org/10.1016/j.psep.2018.06.025.
[13] Samadi, M., Sarikhani, N. Zirak, M., Zhang, H.L.H.H.L., Moshfegh, A.Z., (2018). Group 6 transition metal dichalcogenide nanomaterials: Synthesis, applications and future perspectives, Nanoscale Horizons 3, 90–204, https://doi.org/10.1039/c7nh00137a.
[14] Krishnan, U., Kaur, M., Kaur, G., Singh, K., Dogra, A.R., Kumar, M., Kumar, A. (2019). MoS_2/ZnO nanocomposites for efficient photocatalytic degradation of industrial pollutants, Mater Res Bull 111, 212–221, https://doi.org/10.1016/j.materresbull.2018.11.029.
[15] Tian, Q., Wu, W., Yang, S., Liu, J., Yao, W., Ren, F., Jiang, C. (2017). Zinc Oxide Coating Effect for the Dye Removal and Photocatalytic Mechanisms of Flower-Like MoS_2 Nanoparticles, Nanoscale Res Lett 12, 1–10, https://doi.org/10.1186/s11671-017-2005-0.
[16] Benavente, E., Durán, F., Sotomayor-Torres, C., González, G. (2018). Heterostructured layered hybrid ZnO/MoS_2 nanosheets with enhanced visible light Photocatalytic activity, J Phys Chem Solids 113, 119–124, https://doi.org/10.1016/j.jpcs.2017.10.027.
[17] Rahimi, K., Moradi, M., Dehghan, R., Yazdani, A. (2019). Enhancement of sunlight-induced photocatalytic activity of ZnO nanorods by few-layer MoS_2 nanosheets, Mater Lett 234 134–137, https://doi.org/10.1016/j.matlet.2018.09.103.
[18] Selvaraj, R., Kalimuthu, K.R., Kalimuthu, V. (2019). A type-II MoS_2/ZnO heterostructure with enhanced photocatalytic activity, Mater Lett 243 183–186, https://doi.org/10.1016/j.matlet.2019.02.022.
[19] Jian, W., Cheng, X., Huang, Y., You, Y., Zhou, R., Sun, T., Xu, J. (2017). Arrays of ZnO/MoS_2 nanocables and MoS_2 nanotubes with phase engineering for bifunctional photoelectrochemical and electrochemical water splitting, Chem Eng J 328, 474–483, https://doi.org/10.1016/j.cej.2017.07.056.
[20] Li, H., Shen, H., Duan, L., Liu, R., Li, Q., Zhang, Q., Zhao, X. (2018). Enhanced Photocatalytic activity and synthesis of ZnO nanorods/MoS_2composites, Superlattices Microstruct 117, 336–341, https://doi.org/10.1016/j.spmi.2018.03.028.

[21] Wang, G., Yuan, H., Chang, J., Wang, B., Kuang, A., Chen, H. (2018). ZnO/MoX_2 (X = S, Se) composites used for visible light photocatalysis, RSC Adv. 8, 10828–10835, https://doi.org/10.1039/C7RA10425A.
[22] Wang, S., Ren, C., Tian, H., Yu, J., Sun, M. (2018). MoS_2/ZnO van der Waals heterostructure as a high-efciency water splitting photocatalyst: A frst-principles study, Phys Chem Chem Phys 20, 13394–13399, https://doi.org/10.1039/c8cp00808f.
[23] Kargar, A., Partokia, S.S., Niu, M.T., Allameh, P., Yang, M., May, S., Cheung, J.S., Sun, K., Xu, K., Wang, D. (2014). Solution-grown 3D Cu_2O networks for efficient solar water splitting, Nanotechnology 25 (20) 205401.
[24] Mahmoud, M.A., Qian, W., El-Sayed, M.A. (2011). Following charge separation on the nanoscale in Cu_2O-Au nanoframe hollow nanoparticles, Nano Lett. 11 (8) 3285-3289.
[25] Zhang, Z., Wang, P. (2012). Highly stable copper oxide composite as an effective photocathode for water splitting via a facile electrochemical synthesis strategy, J. Mater. Chem. 22 (6) 2456-2464.
[26] Paracchino, A., Laporte, V., Sivula, K., Gratzel, M., Thimsen, E. (2011). Highly active oxide photocathode for photoelectrochemical water reduction, Nat. Mater. 10 (6) 456-461.
[27] Bai, J., Li, Y., Wang, R., Huang, K., Zeng, Q., Li, J., Zhou, B. (2015). A novel 3D ZnO/Cu_2O nanowire photocathode material with highly efficient photoelectrocatalytic performance, J. Mater. Chem. 3 (45) 22996-23002.
[28] Cushing, S.K., Li, J., Meng, F., Senty, T.R., Suri, S., Zhi, M., Li, M., Bristow, A.D., Wu, N., (2012). Photocatalytic activity enhanced by plasmonic resonant energy transfer from metal to semiconductor, J. Am. Chem. Soc. 134 (36) 15033-15041.
[29] Wang, G., Wang, H., Ling, Y., Tang, Y., Yang, X., Fitzmorris, R.C., Wang, C., Zhang, J.Z., Li, Y. (2011). Hydrogen-treated TiO_2 nanowire arrays for photoelectrochemical water splitting, Nano Lett. 11 (7) 3026-3033.
[30] Li, H., Li, J., Chen, D., Qiu, Y., Wang, W. (2015). Dual-functional cubic cuprous oxide for non-enzymatic and oxygen-sensitive photoelectrochemical sensing of glucose, Sensor. Actuator. B Chem. 220 441-447.
[31] Zhu, Y., Xu, Z., Yan, K., Zhao, H., Zhang, J. (2017). One-step synthesis of CuO-Cu_2O heterojunction by flame spray pyrolysis for cathodic photoelectrochemical sensing of l-cysteine, ACS Appl. Mater. Interfaces 9 (46) 40452-40460.
[32] Liu, L.X., Fan, G.C., Zhang, J.R., Zhu, J.J. (2018) Ultrasensitive cathode photoelectrochemical immunoassay based on TiO_2 photoanode-enhanced 3D Cu_2O nanowire array photocathode and signal amplification by biocatalytic precipitation, Anal. Chim. Acta 1027 33-40.
[33] Salehmin, M.N.I., Jeffery Minggu, L., Mark-Lee, W.F., Mohamed, M.A., Arifin, K., Jumali, M.H.H., Kassim, M.B. (2018) Highly photoactive Cu_2O nanowire film prepared with modified scalable synthesis method for enhanced photoelectrochemical performance, Sol. Energy Mater. Sol. Cell. 182 237-245.
[34] Zhou, T., Zang, Z., Wei, J., Zheng, J., Hao, J., Ling, F., Tang, X., Fang, L., Zhou, M. (2018) Efficient charge carrier separation and excellent visible light photoresponse in Cu_2O nanowires, Nano Energy 50, 118-125.
[35] Li, R., Zhang, Y., Tu, W., Dai, Z. (2017). Photoelectrochemical bioanalysis platform for cells monitoring based on dual signal amplification using in situ generation of electron acceptor coupled with heterojunction, ACS Appl. Mater. Interfaces 9 (27) 22289-22297.
[36] Zhan, W.W., Kuang, Q., Zhou, J.Z., Kong, X.J., Xie, Z.X., Zheng, L.S. (2013). Semiconductor@ metal-organic framework core-shell heterostructures: a case of ZnO@ZIF-8 nanorods with selective photoelectrochemical response, J. Am. Chem. Soc. 135 (5) 1926-1933.
[37] Zhao, K., Yan, X., Gu, Y., Kang, Z., Bai, Z., Cao, S., Liu, Y., Zhang, X., Zhang, Y. (2016). Selfpowered photoelectrochemical biosensor based on CdS/RGO/ZnO nanowire array heterostructure, Small 12 (2) 245-251.
[38] F.X. Xiao, Z. Zeng, B. Liu, Bridging the gap: electron relay and plasmonic sensitization of metal nanocrystals for metal clusters, J. Am. Chem. Soc. 137 (33) (2015) 10735-10744.
[39] Shaislamov, U., Krishnamoorthy, K., Kim, S.J., Chun, W., Lee, H.J. (2016). Facile fabrication and photoelectrochemical properties of a CuO nanorod photocathode with a ZnO nanobranch protective layer, RSC Adv. 6 (105) 103049-103056.
[40] Kargar, A., Jing, Y., Kim, S.J., Riley, C.T., Pan, X., Wang, D. (2013). ZnO/CuO heterojunction branched nanowires for photoelectrochemical hydrogen generation, ACS Nano 7 (12) 11112-11120.
[41] Mizuno K, Izaki M, Murase K, Shinagawa T, Chigane M, Inaba M, Tasaka A, Awakura Y. (2005). Structural and electrical characterizations of electrodeposited p-type semiconductor Cu_2O films. J Electrochem Soc;152:C179-82.
[42] Akimoto K, Ishizuka S, Yanagita M, Nawa Y, Paul GK, Sakurai T. (2006). Thin film deposition of Cu_2O and application for solar cells. Sol Energy;80:715-22.

[43] Sharma D, Satsangi VR, Shrivastau R, Waghmare UV, Dass S. (2016). Understanding the photoelectrochemical properties of nanostructured CeO_2/Cu_2O heterojunction photoanode for efficient photoelectrochemical water splitting. Int J Hydrogen Energy;41:18339-50.
[44] Yao LZ, Wang WZ, Wang LJ, Liang YJ, Fu JL, Shi HL. (2018). Chemical bath deposition synthesis of TiO_2/Cu_2O core/shell nanowire arrays with enhanced photoelectrochemical water splitting for H-2 evolution and photostability. Int J Hydrogen Energy;43:15907-17.
[45] Jung S, Yong K. (2011). Fabrication of CuO-ZnO nanowires on a stainless steel mesh for highly efficient Photocatalytic applications. Chem Commun;47:2643-5.
[46] Erdogan IY. (2010). The alloying effects on the structural and optical properties of nanocrystalline copper zinc oxide thin films fabricated by spin coating and annealing method. J Alloy Comp;502:445-50.
[47] Sisman I, Tekir O, Karaca H. (2017). Role of ZnO photoanode nanostructures and sensitizer deposition approaches on the photovoltaic properties of CdS/CdSe and CdS1-xSex quantum dot-sensitized solar cells. J Power Sources;340:192-200.
[48] Zhang YC, Tang JY, Wang GL, Zhang M, Hu XY. (2006). Facile synthesis of submicron Cu_2O and CuO crystallites from a solid metal organic molecular precursor. J Cryst Growth;294:278-82.
[49] Johan MR, Suan MSM, Hawari NL, Ching HA. (2011). Annealing effects on the properties of copper oxide thin films prepared by chemical deposition. Int J Electrochem Sci;6:6094-104.
[50]. Wang, Q.; Lei, Y.; Wang, Y.; Liu, Y.; Song, C.; Zeng, J.; Song, Y.; Duan, X.; Wang, D.; Li, Y. (2020) Atomic-scale engineering of chemicalvapor-deposition-grown 2D transition metal dichalcogenides for electrocatalysis. *Energy Environ. Sci. 13*, 1593–1616, https://doi.org/10.1039/d0ee00450b.
[51]. Najmaei, S.; Liu, Z.; Zhou, W.; Zou, X.; Shi, G.; Lei, S.; Yakobson, B.I.; Idrobo, J.C.; Ajayan, P.M.; Lou, J. (2013)Vapour phase growth and grain boundary structure of molybdenum disulphide atomic layers. *Nat. Mater.*, *12*, 754–759, https://doi.org/10.1038/nmat3673.
[52] Meng, L., Li, Y., Yang, R., Zhang, X., Du, C., Chen, J. (2019). A sensitive photoelectrochemical assay of miRNA-155 based on a CdSe QDs//NPC-ZnO polyhedra photocurrent-direction switching system and target-triggered strand displacement amplification strategy, Chem. Commun. 55 (15) 2182-2185
[53] Almeida B.M., Melo Jr M.A., Bettini J., Benedetti J.E., Nogueira A.F. (2015). A novel nanocomposite based on TiO_2/Cu_2O/reduced graphene oxide with enhanced solar-light-driven photocatalytic activity, Appl. Surf. Sci. 324, 419–431.
[54] Ganesan K. P., Anandhan N. Marimuthu T. Panneerselvam R. A. Amali Roselin. (2018). Effect of Deposition Potential on Synthesis, Structural, Morphological and Photoconductivity Response of Cu2O Thin Films by Electrodeposition Technique. Acta Metallurgica Sinica (English Letters) https://doi.org/10.1007/s40195-019-00876-5
[55] Quan-Bao Ma n, Jan P. Hofmann, Anton Litke, Emiel J.M. Hensen. (2015). Cu2O photoelectrodes for solar water splitting: Tuning photoelectrochemical performance by controlled faceting. Solar Energy Materials & Solar Cells 141 (2015) 178–186. http://dx.doi.org/10.1016/j.solmat.2015.05.025
[56] Bharathi V, Sivakumar M, Udayabhaskar R, Takebe H, Karthikeyan B. (2014). Optical, structural, enhanced local vibrational and fluorescence properties in K-doped ZnO nanostructures. Appl Phys A;116:395-401.
[57] Ghosh M, Dilawar N, Bandyopadhyay AK, Raychaudhuri AK. (2009). Phonon dynamics of Zn(Mg,Cd)O alloy nanostructures and their phase segregation. J Appl Phys;106, 084306.
[58] Bhosale MA, Bhanage BM. (2016). A simple approach for sonochemical synthesis of Cu_2O nanoparticles with high catalytic properties. Adv Powder Technol;27:238-44.
[59] Guo D, Wang L, Du Y, Ma Z, Shen L. (2015). Preparation of octahedral Cu_2O nanoparticles by a green route. Mater Lett;160:541-3.
[60] Nandiyanto, A. B. D., Andika, R., Aziz, M., and Riza, L. S. (2018). Working Volume and MillingTime on the Product Size/Morphology, Product Yield, and Electricity Consumption inthe Ball-Milling Process of Organic Material. *Indonesian Journal of Science andTechnology*, 3(2), 82-94.
[61] Zhang, Y.; Chen, P.; Wen, F.; Huang, C.; Wang, H. (2016). Construction of polyaniline/ molybdenum sulfide nanocomposite: Characterization and its electrocatalytic performance on nitrite. Ionics, 22, 1095–1102.
[62] Zhang, Y.; Chen, P.; Wen, F.; Huang, C.; Wang, H. (2016). Construction of polyaniline/ molybdenum sulfide nanocomposite: Characterization and its electrocatalytic performance on nitrite. Ionics, 22, 1095–1102.
[63] Jaleel, U.C.; Devi, K.R.; Madhushree, P. (2021). Statistical and Experimental Studies of $MoS_2/g\text{-}C_3N_4/TiO_2$: A Ternary Z-Scheme Hybrid Composite. *J. Mater. Sci.*, *56*, 6922–6944.